JOURNAL OF MATERIALS SCIENCE: MATERIALS IN MEDICINE 5 (1994) 214–218

Measurement of the elastic modulus of fibre-reinforced composites used as orthodontic wires

J. JANCAR, A. T. DIBENEDETTO
Institute of Materials Science, University of Connecticut, Storrs, CT 06269-3136, USA
Y. HADZIINIKOLAU, A. J. GOLDBERG
University of Connecticut Health Center, Farmington, CT 06030, USA
A. DIANSELMO
ISRIM, Terni, Italy

The mechanical properties of an orthodontic wire pultruded from S2-glass-reinforced polyethyleneterephthalate glycol (PETG) were measured using two experimental devices simulating clinical conditions. A comparison of moduli measured in the clinically relevant devices with those measured in a standard flexural test reveals that data obtained using small cross-section, short span length clinical specimens require corrections associated with clamping and shearing effects. The clamping effect dominates and is caused by the softening of the material near the clamps. The shear effect becomes important at high fibre volume fractions and small span/thickness ratios. With adoption of these corrections, good agreement between moduli calculated using rule of mixtures and those measured in clinical tests is achieved. The analytical base developed for prediction of the stiffness of the orthodontic wire for different span/thickness ratios improves the procedure for design of dental appliances.

1. Introduction

Continuous fibre-reinforced plastics (FRP) are widely used in many aerospace, automotive and recreational applications, primarily because of their high stiffness and strength per unit weight. The growing availability of various polymer matrices, reinforcing fibres and processing techniques, as well as the decreasing cost, offer new design opportunities in other fields. A control of material behavior, the potential for *in situ* forming of an appliance in a clinical setting, the ability to bond directly to a tooth structure and the fabrication of translucent, esthetic devices, make glass fiber-reinforced composites attractive candidates as structural components for dental applications. They can be successfully adapted to a number of dental uses, such as frameworks for provisional bridges, splints, retainers, space maintainers and orthodontic wires, either as substitute materials in currently used devices or as a means of creating novel designs.

The use of fibre-reinforced composites has been described in the dental literature for at least 30 years. However, while virtually all reports show positive results, fibre reinforcement has not been successfully reduced to clinical practice [1]. This is probably due to low fibre loading, ineffective stress transfer to the reinforcement, and demanding manipulative procedures in the clinical setting. Recent work demonstrated that the use of pultruded thermoplastic prepregs may obviate these problems [1–3].

Cricital to the development of FRC for dental applications are adequate characterization and prediction of flexural properties (modulus, strength, strain) and reliable design procedures. Even though an orthodontic wire is "monodimensional" in the sense that its length is many orders of magnitude greater than its cross-section, the anisotropic nature of FRC wires insures that the transverse (radial) properties of the wire are as important to their mechanical performance as are the longitudinal (axial) properties. While the longitudinal properties define the tensile strength and stiffness of the wire, the transverse properties control the shear strength and the long term stability of the device in the oral environment. Structural components in orthodontic appliances are stressed mainly in flexure. Standard flexural tests (3- or 4-point bending) are based on long beam theory [4], assuming free beam ends, and they do not provide an accurate means of determining intrinsic properties of specimens with a small span length/thickness ratio (L/d) and clamped at one or both ends. Thus, an experimental procedure to simulate clinical conditions using small cross-section, short span length and clamped specimens is required. Novel testing devices have been developed to provide both clinically relevant data and material intrinsic properties [5, 6].

The aim of this study is to provide an analytical base for evaluation of the intrinsic mechanical properties of unidirectional long fibre composite wires from

0957–4530

experimental data obtained in tests on clinically relevant specimens. The effect of the fibre volume fraction and specimen geometry on the elastic modulus is investigated. Analytical relations between the load–deflection data of the orthodontic wire tested in two clinically relevant devices and the intrinsic mechanical characteristics of the composite are developed using a short beam theory [7] for the two different loading geometries.

2. Materials and methods

Continuous S2-glass fiber-reinforced polyethyleneterephthalate glycol (PETG Copolyester 67743; Eastman Chemical Products, Kingsport, TN, USA) wires were pultruded to nominal cross-sectional dimensions of 0.483 mm × 0.635 mm at Polymer Composites, Inc. (Winona, MN, USA). The S2- glass fibres were coated with glycidoxy-propyltrimethoxy silane A187 of Union Carbide (Danbury, CT, USA). The fibre volume fraction of the wire was determined from the weight fraction after ashing. Fibre content ranged between 40% and 60% by volume.

The elastic modulus of the pultruded composite wire and unreinforced PETG were measured with the devices shown in Fig. 1. In device I, the specimen was clamped rigidly at one end and simply supported at the other (Fig. 1a). A moment is applied at the clamped end and the deflection is recorded as a function of applied moment for a given span length. A torque watch (Waters Manufacturing, MA, USA) was used to measure the moment and a dial gauge was used to record the angular rotation. Clinically relevant span lengths from 0.5 to 3.0 cm (L/d ratio from 10 to 60) were tested. To simulate the actual clinical situation, a two bracket step geometry deflection apparatus was used (Fig. 1b). A sample wire was loaded into the brackets in an even and parallel position with span lengths of 5 and 10 mm (L/d ratio of 10 and 20). One of the brackets was then deflected in increments of 0.1 mm with the brackets remaining parallel throughout the test. At each increment of deflection, a force transducer read from the deflecting bracket the vertical and horizontal forces and input these data into a computer. Tests were performed at room temperature.

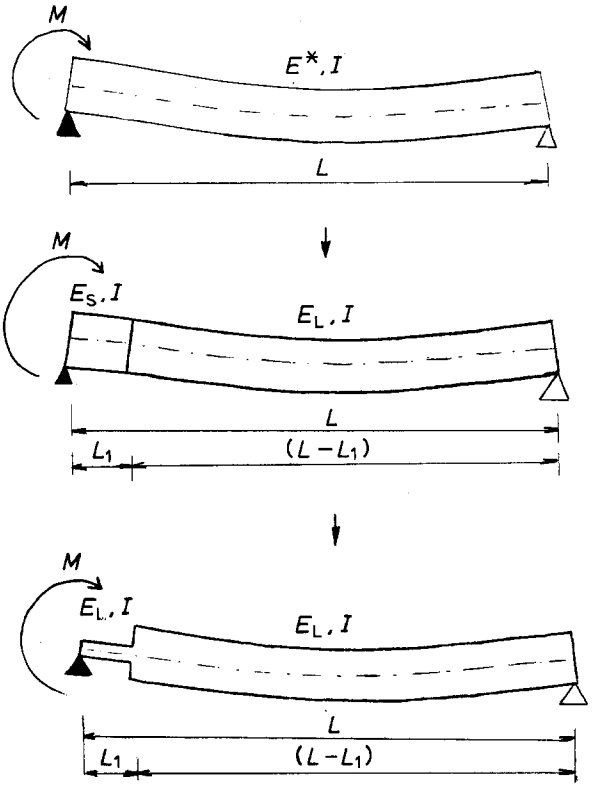

Figure 1a Schematic representation of device I. Symbols described in the text.

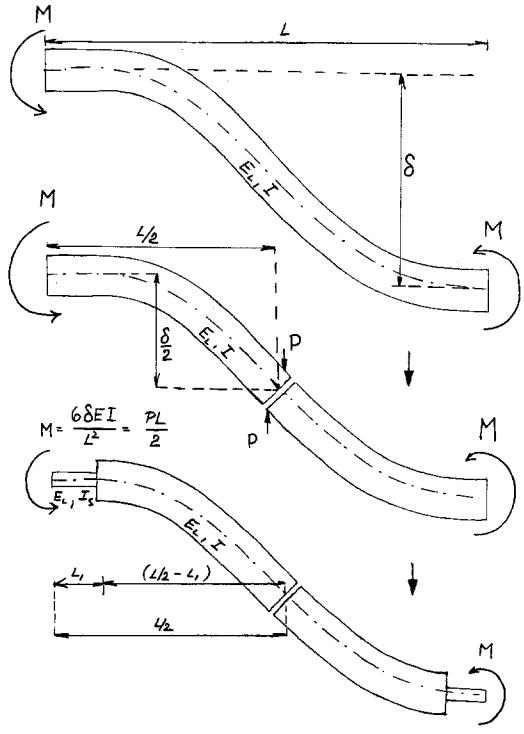

Figure 1b Schematic representation of device II. Symbols described in the text.

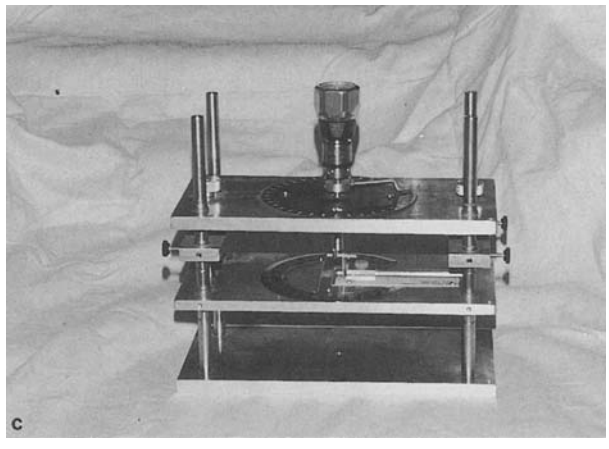

Figure 1c Photograph of device I.

Large samples for standard flexural tests were prepared by a filament winding procedure by passing a bundle of treated fibres through a solution of PETG in chloroform and winding the coated fibres on a rotating drum. Sheets were then compression moulded out of the wound "prepregs" and specimens for standard flexural tests were cut so that the span length was parallel to the direction of fibres.

3. Results and discussion

For device I, the modulus is determined from the linear portion of the moment–deflection curve using a standard long beam formula [8]:

$$E^* = (1/3)\, LM/\delta I \qquad (1)$$

where L is the beam span length, I is the moment of inertia of the cross-section, M is the applied moment and δ is the associated deflection. For device II, one can calculate the apparent modulus using an expression [9]:

$$E^* = PL^3/(bd^3\,\delta) \qquad (2)$$

where P is the measured force, δ is the associated deflection, b and d are the width and thickness of the beam, respectively, and L is the span length. The measured value of E^* from the clinical devices is referred to as an apparent modulus, since it increases with the span length, approaching asymptotically the value of longitudinal tensile modulus E_L predicted using the rule of mixtures [10]:

$$E_L = E_f v_f + E_m v_m \qquad (3)$$

where E_f and E_m are the fibre and matrix moduli and v_f, v_m are the volume fractions of constituents. Values of E^* as a function of span length are shown in Fig. 2. The asymptotic values of 35 GPa and 48 GPa at 40 and 56 vol% fibre content, respectively, are identical to those predicted from the rule of mixtures using 85 GPa and 2 GPa for the moduli of S-glass and resin, respectively. Values of the longitudinal modulus E_L, determined in the standard flexural test, are in good agreement with the asymptotic values given above.

The dependence of E^* on the span length can be described in terms of the effects of specimen geometry, clamping and shear phenomena. The major contribution to deviations from the true modulus in these devices is from the clamping, which causes a "softening" of the material near the clamp. Our analysis is based on the assumption that beam deflections at the clamp, as well as the clamping itself, cause fibre breakage and matrix yielding. As a result of the fibre fragmentation, the matrix material near the clamp cannot transfer as much load to the fibres and thus the beam appears to be less rigid in this region than in the rest of the beam. The "softened" zone will be no shorter than the beam width, since the yield plane will be at approximately 45–50° to the fibre axis. It may be somewhat longer than this since broken fibre ends will create an "ineffective length" (l_i) over which the fibres cannot be fully loaded [11]. For E-glass fibre well bonded to thermoplastic matrices it has been shown that the "ineffective length" will be of the order of 0.4–0.6 mm [12], which will have a significant effect on the stiffness of typical orthodontic wires.

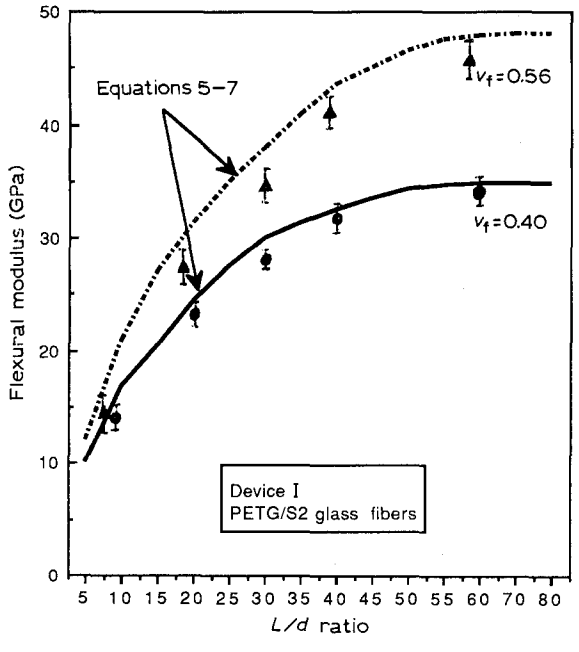

Figure 2a The dependence of the elastic modulus in flexure on the span length/thickness ratio for two S2-glass fibre volume fractions in PETG matrix determined using device I. Points represent experimental data, lines stand for theoretical predictions.

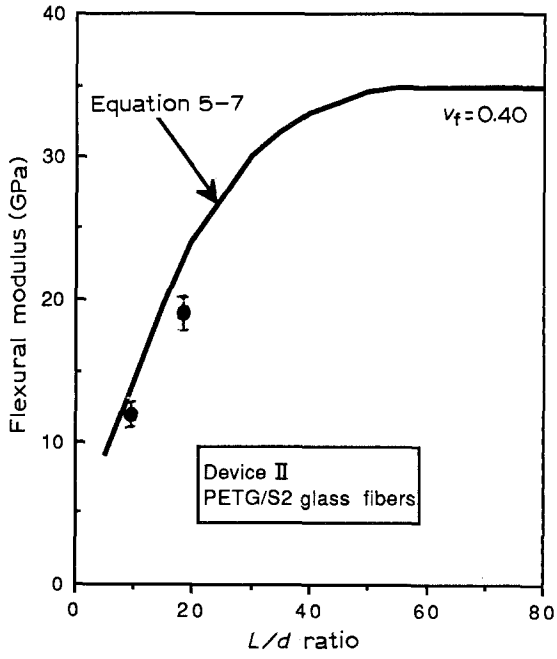

Figure 2b Comparison of the predicted (solid line) and experimental (points) values of elastic moduli in flexure for device II. PETG contains 40 vol % of S2-glass fibres.

Our devices are therefore modeled as composite beams consisting of a "soft" zone of length L_1 and modulus E_s adjacent to the clamp, butted to a rigid zone of length $(L - L_1)$ and modulus E_L, as shown in Fig. 1. The length L_1 will be equal to the larger of beam thickness, d, or the ineffective length, L_i. This composite beam can be analyzed utilizing the principle of equivalent sections by replacing the "soft" zone with a "rigid" zone of cross-section area given by [13]:

$$A_{rigid} = (E_{soft}/E_{rigid})\, A_{soft} \qquad (4)$$

In terms of the moments of inertia of a rectangular beam of unit width:

$$I_{rigid}/I_{soft} = (d_{rigid}/d_{soft})^3 = (E_{soft}/E_{rigid})^3 \qquad (5)$$

This is shown schematically in Fig. 1 and the analysis is summarized briefly in Appendices A and B.

The relationship between the true elastic modulus E_L and the apparent one E_L^* can be expressed as:

$$E_L = C\, E_L^* \qquad (6)$$

where the correction factor C^{I} for a glass fibre-reinforced composite beam in device I is given as (Appendix A):

$$C^{I} = \{(1 + (I/I_s - 1)[3/2(d/L) - 1/2(d/L)^2]\} \times \{1 - 3/8(E_L/G)(d/L)^2\}^{-1} \quad (7)$$

and C^{II} for device II is given as (Appendix B):

$$C^{II} = \{(1 + 12(I/I_s - 1)[1/2(d/L) - (d/L)^2 + 2/3(d/L)^3]\} \times \{1 - 3/2(E_L/G)(d/L)^2\}^{-1} \quad (8)$$

where I and I_s are the moments of inertia of the rigid and soft portion of the beam, respectively, d and L are beam thickness and span length and G is the in-plane shear modulus measured in an independent experiment. The shear correction only accounts for less than 10%.

A fitting of the experimental data for both geometries with proposed analytical expressions (Equations 6–8) yields the empirical parameter (I/I_s) equal to about 7.5 for device I and about 5 for device II. From Equation 5 one can calculate the modulus of the soft zone near the clamp to be about 0.5 of that for the remainder of the beam, which is consistent with the notion that the clamped end behaves as a short (broken) fibre composite [14].

The shear correction becomes relatively more important with increasing fibre volume fraction, especially in the case of a weak matrix–fibre interface. After making these two corrections the modulus obtained from data on the clinically relevant specimens is within 10% of the intrinsic value of E_L predicted using the rule of mixtures at all span to depth ratios studied. This discrepancy may be attributed to the difference between the compressive and tensile modulus of the material [15–17] and/or to the simplifying assumptions of the mechanical analysis.

4. Conclusions

When using continuous glass fibre-reinforced thermoplastics as orthodontic wires, the intrinsic stiffness of the material cannot be fully utilized. Short beam lengths, clamped ends and relatively high flexural deformations at the clamps lead to shear effects and fibre damage that reduce the rigidity of the appliance. Two experimental devices have been used to simulate clinical use of orthodontic wires. The apparent beam stiffnesses obtained in the devices have been measured and analytical models developed to relate the results to the intrinsic properties of the beam. It appears that within a distance from the clamps of roughly either the thickness of the beam or the ineffective fibre length in the composite, the stiffness can be reduced to about one half that of the remainder of the wire. This is indicative of fibre breakage and matrix shearing near the clamps. The information provided in this work should be useful in the design of dental appliances made of continuous fibre-reinforced plastics.

Appendix A

The relation between the tensile modulus (E_L) and the apparent modulus (E^*) can be obtained from the differential equations for the elastic deformation of the composite beam. For our system we assume that the soft zone has a length equal to beam thickness, $L_i = d$. Referring to Fig. 1a, one can write the differential equations for the beam as [13]:

$$E^* I(d^2y/dx^2) = M(1 - x/L) \text{ for } 0 < x < L \quad (A1)$$

with boundary conditions $y = 0$ at $x = 0$, $x = L$, and for the equivalent beam as:

$$E_L I_s(d^2y/dx^2) = M(1 - x/L) \text{ for } 0 < x < d, \quad (A2)$$

with boundary conditions $y = 0$ at $x = 0$ and $y = y_B$ at $x = d$ and

$$E_L I(d^2y/dx^2) = M(1 - x/L) \text{ for } d < x < L \quad (A3)$$

with boundary conditions $y = y_B$ at $x = d$ and $y = 0$ at $x = L$, where $(E_L I_s)$ and $(E_L I)$ are the flexural rigidities of the two zones, M is the applied bending moment, and L and d are the span length and beam thickness, respectively. Solving the above equations under the boundary and continuity conditions and comparing the solution for the equivalent beam with that for the homogeneous beam, one can determine a relation between the corrected modulus E_L and the apparent one E_L^*:

$$E_L = \{(1 + (I/I_s - 1)[3/2(d/L) - 1/2(d/L)^2]\} \times E_L^* \quad (A4)$$

for device I. As (d/L) approaches zero, i.e. for long beams, the apparent modulus reaches the true longitudinal Young's modulus E_L predicted by the rule of mixtures:

$$E_L = E_f v_f + E_m v_m \quad (A5)$$

where E_f, E_m are the fibre and matrix moduli, respectively, and v_f, v_m are the component volume fractions.

The shear correction can be simply accounted using an expression commonly utilized [19]:

$$E_L = \{1 - (3/8)(E_L/G)(d/L)^2\}^{-1} \times (E_L)^{\text{uncorr}} \quad (A6)$$

where G is the material shear modulus determined in an independent test. Thus, one can account for both corrections in the resulting expression:

$$E_L = \{(1 + (I/I_s - 1)[3/2(d/L) - 1/2(d/L)^2]\} \times \{1 - 3/8(E_L/G)(d/L)^2\}^{-1} \times E_L^* \quad (A7)$$

for device I.

Young's modulus E_L for a homogeneous solid is equal to the flexural modulus E_L^{flex} only in the case when compressive and tensile moduli are equal [14]. Also, for long fiber-reinforced composites, the flexural modulus measured in a 3-point bending test is higher than the tensile modulus because of the length dependence of fibre strength. For glass-reinforced composites, the relation between flexural and tensile moduli can be estimated by [13]:

$$E_L^{\text{flex}} = \{[2(1 + m)]^{1/m}\} E_L \approx 1.64 E_L \quad (A8)$$

where m is the Weibull dispersion parameter for the fibres [18].

Appendix B

A similar procedure to that in Appendix A can be used to evaluate the effect of clamping for device II (Fig. 1b). The homogeneous beam is substituted by a pair of matched cantilever beams undergoing equal deformation. Each cantilever can then be replaced by an equivalent composite beam with the length of softened zone near the clamps equal to d. In this case, the force P is measured for any deflection. Then the basic beam equations can be written as [9]:

$$E^* I(d^2y/dx^2) = PL/2\,[1 - 2x/L] \quad \text{for } 0 < x < L/2 \tag{B1}$$

with boundary conditions $y = 0$, $dy/dx = 0$ at $x = 0$,

$$EI_s(d^2y/dx^2) = PL/2\,[1 - 2x/L] \quad \text{for } 0 < x < d \tag{B2}$$

with boundary conditions $y = 0$, $dy/dx = 0$ at $x = 0$, $y = y_B$ at $x = d$ and

$$EI(d^2y/dx^2) = PL/2\,[1 - 2x/L] \quad \text{for } d < x < L/2 \tag{B3}$$

with boundary conditions $y = \delta/2$ at $x = L/2$, $y = y_B$ at $x = d$. Solving Equations B1–B3 using appropriate boundary and continuity conditions and comparing the solution for the composed beam with that for a homogeneous beam, one can obtain the relationship between the intrinsic elastic modulus for the glass fibre-reinforced beam and the apparent one:

$$E_L = \{(1 + 12(I/I_s - 1)[1/2(d/L) - (d/L)^2 + 2/3(d/L)^3]\}E_L^* \tag{B4}$$

Accounting for the shear effect, one obtains a final expression for the longitudinal elastic modulus from the values obtained with clinical device II:

$$E_L = \{(1 + 12(I/I_s - 1)[1/2(d/L) - (d/L)^2 + 2/3(d/L)^3]\} \times \{1 - (3/2)(E_L/G)(d/L)^2\}^{-1} \times E_L^* \tag{B5}$$

Acknowledgements

The authors wish to thank to Professor Charles J. Burstone, Department of Orthodontics, for information on clinical application of the FRC wires and Dr Douglas A. Rollins for providing some experimental data on device II. The work was supported by the NIH Grant no. DE 09126-02, which is also acknowledged.

References

1. A. J. GOLDBERG and C. J. BURSTONE, *J. Dent. Mater.* in press (1992).
2. A. J. GOLDBERG, C. J. BURSTONE and H. A. KOENIG, *J. Dent. Res.* **62** (1983) 1016.
3. P. J. HENRY, B. M. BISHOP and R. M. PURT, *Quint. Dent. Technol.* **1990/1991** (1991) 110.
4. S. TIMOSHENKO, "Strength of materials", vol. 1, 2nd Edn (van Nostrand, New York, 1940) p. 170.
5. Y. HADZIINIKOLAU, PhD Thesis (1992).
6. D. A. ROLLINS, Research paper, Department of Orthodontics, University of Conn. Health Center, Farmington (1989).
7. Y. C. KU, "Deflections of beams for all spans and cross sections" (McGraw-Hill, New York, 1986) p. 136.
8. P. P. BENHAM and R. J. CRAWFORD, "Mechanics of engineering materials", Ch. 7 (J. Wiley & Sons, New York, 1987) p. 172.
9. *Idem, ibid.* p. 216.
10. L. J. BROUTMAN and B. D. AGARWAL, "Analysis and performance of fiber composites" (J. Wiley & Sons, New York, 1980) p. 22.
11. A. KELLY and W. R. TYSON, *J. Mech. Phys. Solids* **13** (1965) 329.
12. A. T. DiBENEDETTO, *Composite Sci. Technol.* **42** (1991) 103.
13. F. L. SINGER, "Strength of materials", Ch. 10 (Harper & Bros., New York, 1951) p. 329.
14. J. HALPIN and J. L. KARDOS, *Polym. Eng. Sci.* **16** (1976) 344.
15. J. G. WILLIAMS, "Stress analysis of polymers", Ch. 4 (J. Wiley & Sons, New York, 1973) p. 113.
16. T. V. PARRY and A. S. WRONSKI, *J. Mater. Sci.* **16** (1981) 439.
17. L. J. BROUTMAN and B. D. AGARWAL, "Analysis and performance of fiber composites" (J. Wiley & Sons, New York, 1980) p. 58.
18. D. HULL, "An introduction to composite materials", Ch. 7 (Cambridge University Press, Cambridge, 1981) p. 125.
19. S. TIMOSHENKO and J. N. GOODDIER, "Theory of elasticity", 2nd Edn (McGraw-Hill, New York, 1951) p. 39.

Received 8 June 1992
and accepted 1 February 1993